NAIC-ID(RS)T-0759-94

NATIONAL AIR INTELLIGENCE CENTER

ELECTRIC FIELD-ASSISTED DEPOSITION OF
ZnS/Na_3AlF_6 INTERFERENCE FILTERS

by

Gu Peifu

NAIC- ID(RS)T-0759-94

HUMAN TRANSLATION

NAIC-ID(RS)T-0759-94 19 April 1995

MICROFICHE NR: 95C000249

ELECTRIC FIELD-ASSISTED DEPOSITION OF
ZnS/Na_3AlF_6 INTERFERENCE FILTERS

By: Gu Peifu

English pages: 13

Source: Guangxue Xuebao, Vol. 5, Nr. 1, January 1985;
pp. 50-54

Country of origin: China
Translated by: Leo Kanner Associates
F33657-88-D-2188
Requester: NAIC/TATD/Bruce Armstrong
Approved for public release; Distribution unlimited.

THIS TRANSLATION IS A RENDITION OF THE ORIGINAL FOREIGN TEXT WITHOUT ANY ANALYTICAL OR EDITORIAL COMMENT STATEMENTS OR THEORIES ADVOCATED OR IMPLIED ARE THOSE OF THE SOURCE AND DO NOT NECESSARILY REFLECT THE POSITION OR OPINION OF THE NATIONAL AIR INTELLIGENCE CENTER.	PREPARED BY: TRANSLATION SERVICES NATIONAL AIR INTELLIGENCE CENTER WPAFB, OHIO

GRAPHICS DISCLAIMER

All figures, graphics, tables, equations, etc. merged into this translation were extracted from the best quality copy available.

ELECTRIC FIELD-ASSISTED DEPOSITION OF ZnS/Na_3AlF_6 INTERFERENCE FILTERS

Gu Peifu, Department of Optical Instrumentation, Zhejiang University, Hangzhou

Abstract: If an appropriate electric field is applied during the deposition of narrow-band interference filters, optical stability can be improved. In this article, AC or DC electric fields have been used to prepare ZnS/cryolite filters. As a result, the measured peak transmission wavelength basically remains constant even at 100% relative humidity. Some reasons for the improved filter stability are also analyzed.

I. Introduction

Optical light spectral instability of narrow-band interference filters brings many difficulties to practical applications. Therefore, a great deal of research was conducted for many years. At a very early time, Schildt et al. [1] proposed that filter wavelength drift is related to vapor

pressure, and the drift is due to infiltration of moisture into the separation layer. Livina and Furman [2] also pointed out that filter properties have a delayed phenomenon when temperature changes due to moisture infiltrating the filter. They also said that unless the edges of filters are carefully sealed, moisture infiltration is still unavoidable even into cemented filters. The most persuasive is perhaps an experiment conducted by Macleod et al. [3]. They carefully observed the infiltration process of moisture into the filters, and then analyzed the relationship between changing transmission peaks and moisture adhesion.

After researchers realized that moisture infiltration is the main reason for drifting filter wavelengths, many measures to stabilize filter properties successively appeared. For example, considering that the separation layer is the most sensitive to the effects of drifting, the higher aggregate density ZnS is used as the separation layer. Or, the researchers engaged in cementing and sealing of edges so that satisfactory separation was maintained between the film layer and the atmosphere. However, these methods have not solved the basic point. Martin et al. [4] directly started by raising the aggregate density of the film layer; in the deposition process, incessant ion bombardment was applied to the film layer so that the filter drift composed of ZrO_2/SiO_2 is reduced from 8 to 0.6nm. The

author and his colleagues pursued another route; in the deposition process, an appropriate horizontal electric field was applied so that the peak value wavelength of the most common ZnS/Na_3AlF_6 interference filter was stabilized within the range of the limiting precision (plus or minus 5Angstroms) as measured instrumentally.

II. Description of Experiment

This experiment was accomplished with a DMD-450 film coating machine. A high AC potential of 3200 to 3400V or a high DC potential of about 2500V was applied with an ion bombardment transformer. The electrodes were placed beneath the lens disk approximately at a distance of 40mm as shown in Fig. 1. High-current, high-voltage electrodes were two aluminum semicircles; the DC electrode was an aluminum ring with a diameter of about 180mm.

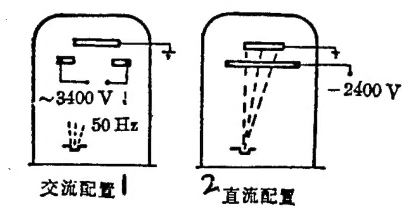

Fig. 1. Arrangement of electrodes in vacuum chamber
KEY: 1 - AC layout 2 - DC layout

Considering that the most widely applied, at present, is narrow-band interference filters coated with ZnS/Na_3AlF_6. Moreover, the drift of the filter's center wavelength depends on

the levels and numbers of layers of reflective pile. In general situations, drifting of separation layer with low reflective index is at least several times higher than that of the separation layer with high reflective index. To facilitate observation of comparative results, the filter structure is selected as

$$G(HL)^2H4LH(LH)^2A \qquad (1)$$

in (1), H is ZnS and L is Na_3AlF_6. ZnS is a gas-phase bulk material; while cryolite is hot-pressed bulk material. An electron beam is used for evaporation. The temperature of the substrate was at room temperature. During evaporation, the dynamic vacuum was $5x10^{-5}$torr. For a quarter-wavelength film of 560nm control wavelength, the evaporation time was approximately 40s.

The light-splitting curve of the filter was measured with a UV-VIS spectrophotometer. During discharge, the vacuum chamber is filled with dry air. In order to accelerate the filter experiment, the most undesirable environment was chosen. In other words, the not-yet-grown filters were directly exposed in a container at 100% relative humidity, then the light splitting transmission property was measured at definite periods of time.

III. Experimental Results

In the deposition process, after the two above-mentioned forms of electric field were applied in the vacuum chamber, the fabricated filters were very stable.

Important is the comparison with filters with no electric field application. As found by visual observation, such filters are not observed with moisture absorption spots even at 100% relative humidity. Fig. 2 shows the variation in moisture infiltration spots at 100% relative humidity for filters prepared without applying an electric field. These pictures were photographed with a simple camera. Based on variation in infiltrated spots, it can be estimated from the pictures that the difference between the longest and the shortest wavelength is approximately 500-600Angstroms. However, for filters deposited with the application of an electric field, no such infiltrated spots were observed until the damage to the film layer, reduction in transmissibility and inability of observation occurred.

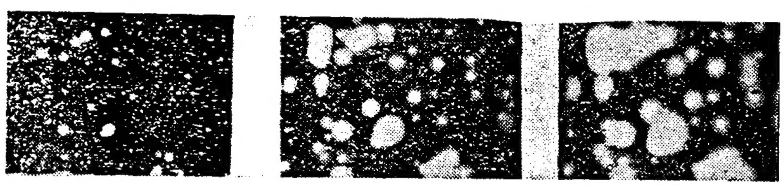

Fig. 2. Penetration patterns of water vapor for conventional filter

With a spectrophotometer for measuring transmissibility curves, no drift of peak-value wavelength was found for filters placed in air for several weeks. Of course, the more strict conditions are experiments at high temperatures. At 100% relative humidity, inspection of filters was conducted from tens

to more than 100 hours. No wavelength drift was basically detected by using a spectrophotometer. Table 1 lists the results of comparative measurements fabricated with the aid of an electric field and with conventional techniques. It is apparent that the wavelength drift of filters fabricated conventionally is alarming. After applying the supplementary electric field, however, almost no drifting was observed. Fig. 3 shows a comparison of the light-splitting curves actually measured. From the figure, moisture corrosion makes very strange final changes in transmissibility for filters fabricated conventionally. After applying an electric field, although some separated curves can be observed at both sides of the filter, yet the drifting of peak-value wavelengths is extremely difficult to be detected.

TABLE 1. Comparative Results of Typical Samples at 100% Relative Humidity

a 常规工艺	t(小时) d	空气中 e	2	5	30	50		
	λ(nm)	561	562	563	~615(双峰)	~620(双峰) f		
	T(%)	88	86.5	75	43 f	44.5		
b 交流电场 (~3400 V, 50 Hz)	t(小时) d	空气中 e	3	19	47	66	99	120
	λ(nm)				561			
	T(%)	88.5	88.5	88	86	84	84	80
c 直流电场 (2400V)	t(小时) d	空气中 e	3	27	42	67	96	
	λ(nm)				561			
	T(%)	88	88	88	88	87	78	

KEY: a - conventional technique b - AC electric field c - DC electric field d - hours e - in air f - two peaks

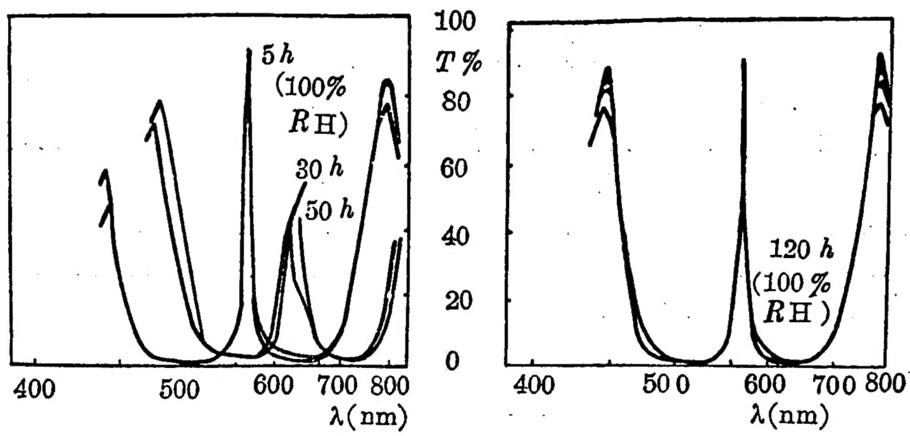

Fig. 3. Measured transmission curves of ZnS/cryolite Air $|(HL)^2H4LH(LH)^2|$ glass deposited on a substrate at room temperature

For filters fabricated with the aid of an electric field, sturdiness of the film layer has also improved, to a certain extent, in addition to increased stability of the light spectrum. Particularly noteworthy is the fact that there are different forms of damage to these two filter types. Densely concentrated small dots appear on the surface of damaged filters prepared with supplementary electric fields; when observed in transmitted light, these spots appear as bright spots, not varying with wavelength. Fig. 4 shows two damaged filters of different wavelength. Although these damaged spots and moisture-absorbing spots are different, the transmission curves for measuring these filters have unchanged center wavelengths; however, the peak-value transmissibility is going down.

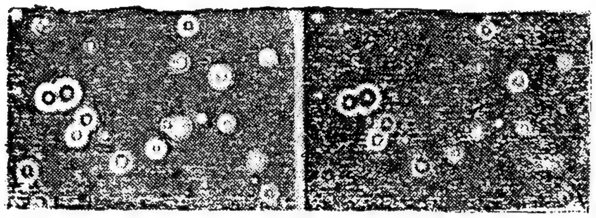

Fig. 4. Photographs of filter damage taken at the peak wavelength and at longer wavelengths of the filter

IV. Analysis and Discussion

To further understand the reason for improved filter stability, the following experiment was conducted by the author and his colleagues.

First, beginning from the measurement of aggregate density, by taking the average value of three experiments, the aggregate density of ZnS was, respectively, 0.93 and 0.98 for two conditions of conventional technique and electric field application; however, the respective aggregate densities of Na_3AlF_6 were 0.82 and 0.9. Based on the aggregation density of measurements, by taking $P_{ZnS}=1$ and $P_{Na_3AlF_6}=0.9$, let us assume that after a filter absorbs moisture for several days at 100% RH, all its pores are filled with water. With computer simulation, it is found that the drift at 560nm wavelength is about 19nm. It is apparent that there is insufficient explanation by using only aggregate density. Of course, there is another possibility: since the aggregate density of ZnS is very steep, this property

can serve as a barrier layer for moisture penetration.

Cryolite film is a very strange material. As reported, the refractive material of the material in bulk is 1.365; however, all refractive indexes of the film layer lie between 1.28 and 1.36. However, we discovered in measurements by using the surface electromagnetic wave method, elliptic deviation method, and the photometric method, the refractive index of cryolite film at 100% humidity can sometimes be as high as 1.45. This explains that possibly certain reactions may exist in cryolite films. Therefore, analyses of Auger spectra were conducted on cryolite films and bulk materials. By comparing Auger spectra of cryolite films and bulk materials evaporated in conventional techniques as shown in Fig. 5, it was found that F and Na are apparently reduced in the film layer; the position of the Al peak is drifted; and the Auger signal O is considerably increased. These results are possibly explained by the existence of large numbers of AlF_3 molecules in the value during higher evaporation rates (such as 25Angstroms per second; thus causing the formation of AlF_4 film. After applying an electric field, the F and Na peaks (especially the F peak) are raised with a relatively large value over that of the film layer in conventional techniques; however, the O peak is reduced somewhat. In other words, these results are closer to those for bulk material constituents. Sine the AlF_3 in $NaAlF_4$ film is higher than that of Na_3AlF_6, we know that

the aggregate density of AlF_3 is much lower than NaF, and also it can lead to $AlF_3 \cdot H_2O$ while the refractive index of $AlF_3 \cdot H_2O$ is 1.49 [5]. Hence, $NaAlF_4$ film exhibits very high instability; its refractive index may even be higher than that of bulk cryolite material.

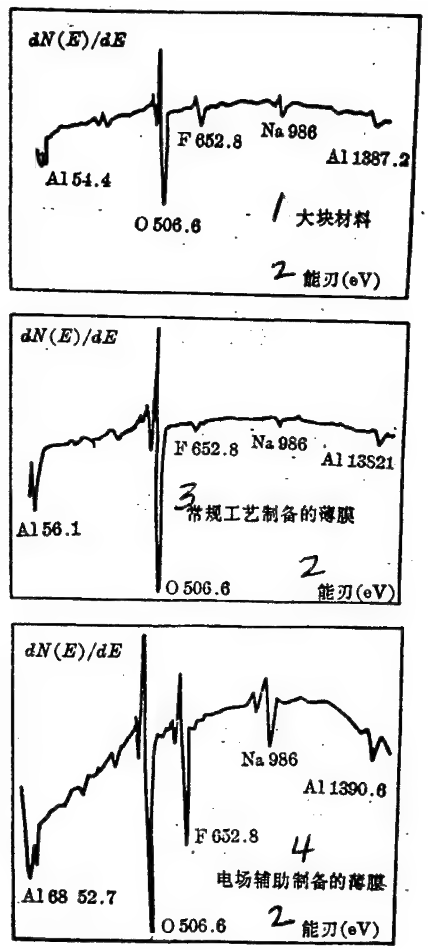

Fig. 5. Auger spectra of cryolite in bulk and in thin films
KEY: 1 - bulk material 2 - energy peak and trough 3 - thin film fabricated with conventional technique 4 - thin film assisted with electric field

Measurement of the properties of the 3micrometer water absorption band may also lead to further understanding of the hydrophilic property of filters. At room temperature, coat film (1) on a sapphire substrate and then place the filter in 100% relative humidity, and measure the property at the 3micrometer band. It was discovered that a small water absorption peak appears near 3micrometers after the filter absorbed water for those filters coated in the conventional way. Conversely, no such phenomenon is observed made with the assistance of an electric field, as shown in Fig. 6.

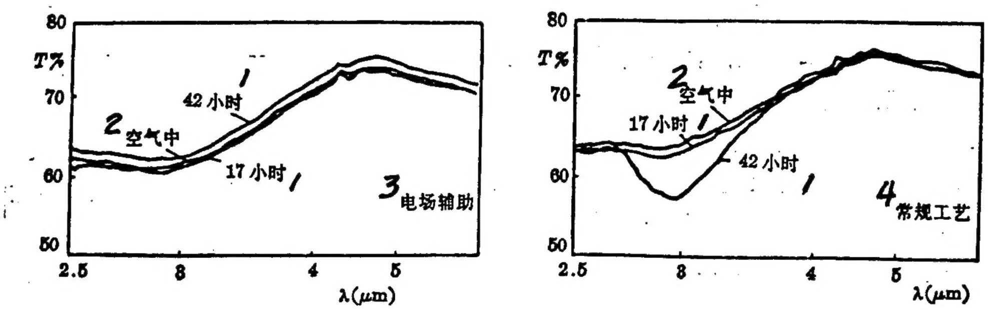

Fig. 6. Measured transmission property of Air |$(HL)^2H4LH(LH)^2$| Al_2O_3 ($lambda_0$=560nm) in 3micrometer water absorption band KEY:1 - hours 2 - in air 3 - electric field-assisted 4 - conventional technique

Some experiments were also conducted on different materials. Under the same electric field, filter (when the filters were composed of different materials) stability showed widely varying differences. For example, the effect is not apparent for

ZnS/MgF_2 filter with the same structure. Generally, the drift is about 100Angstroms for $ZnSe/Na_3AlF_6$ at 100% relative humidity. However, a strange thing occurs: that the peak value wavelength of this filter slowly decreases later on, even approaching the initial wavelength. In addition, the moisture endurance of the film layer is very excellent: the film layer of the specimen is still satisfactory after being placed at 100% relative humidity for 2 months. This explains that different results occur by placing ZnS and Na_3AlF_6 in different film systems. It seems that the stability of ZnS/Na_3AlF_6 filter is a result of the joint contributions of these two materials. Moreover, the effects are not the same by using powdered or bulk cryolite. On filters coated with powdered cryolite, a drift of about 0.2 to 0.3nm can still be observed.

When a material is subjected to re-evaporation, there takes place a complex process of dissolution, distillation, and recombination. When evaporating cryolite, two (positive and negative) electrodes were placed on both sides of the evaporation source, two charge collection electrodes were correspondingly placed at the upper side. It was discovered that there are larger negative charges about the positive electrode; however, although positive charges were not collected above the negative electrode, yet there were very few negative charges. This

explains that there are large quantities of charged particles generated in a vacuum chamber, in addition to neutral particles. This result is consistent with the measurement results by Pulker et al., who used a mass spectrograph. In other words, while ZnS decomposes into single atoms with heated ionization, Na_3AlF_6 is distilled into NaF, AlF_3, and others. Under the function of the electric field, certain dynamic energy may be obtained for ions or polarized molecules, with enhanced consistency of chemical measurements. Since the evaporation-condensation property of different materials are different, it is understandable that the effect is not very obvious for filters composed of other materials.

Finally, the author expresses his gratitude to instruction by teacher Tang Jinfa and assistance by the Auger team.

The article was received for publication on 24 April 1984.

REFERENCES

[1] J. Schild, A. Steudel and H. Walther; *J. De Physique*, 1967, **28**, No. 3~4, (Mar-Apr), C_3, 276.
[2] M. D. Livina and Sh. A. Furman; *Sov. J. Opt. Tech.*, 1973, **4**, No. 3 (Mar), 264.
[3] H. A. Macleod and D. Richmond; *Thin Solid Films*, 1976, **37**, No. 2 (Sep), 163.
[4] P. J. Martin, H. A. Macleod, R. P. Netterfield. C. G. Pacsy and W. G. Sainty; *Appl. Opt.*, 1983, **22**, No. 1, (Jan) 178.
[5] Walter Heitmann; *Thin Solid Films*, 1970, **5**, No. 1 (Jan), 61.

DISTRIBUTION LIST

DISTRIBUTION DIRECT TO RECIPIENT

ORGANIZATION	MICROFICHE
B085 DIA/RTS-2FI	1
C509 BALLOC509 BALLISTIC RES LAB	1
C510 R&T LABS/AVEADCOM	1
C513 ARRADCOM	1
C535 AVRADCOM/TSARCOM	1
C539 TRASANA	1
Q592 FSTC	4
Q619 MSIC REDSTONE	1
Q008 NTIC	1
Q043 AFMIC-IS	1
E051 HQ USAF/INET	1
E404 AEDC/DOF	1
E408 AFWL	1
E410 AFDTC/IN	1
E429 SD/IND	1
P005 DOE/ISA/DDI	1
P050 CIA/OCR/ADD/SD	2
1051 AFIT/LDE	1
P090 NSA/CDB	1
2206 FSL	1

Microfiche Nbr: FTD95C000249
NAIC-ID(RS)T-0759-94